Quantifying Biomolecular Recognition with Site-Specific 2D Infrared Probes

Johnson, Philip J M ; Koziol, Klemens L ; Hamm, Peter

Abstract: Azidohomoalanine (Aha) is an unnatural amino acid containing an infrared active azido side chain group that can, through frequency shifts of the azido stretch vibration, act as a probe of local structure. To realize the potential of such structural probes for protein science, we have developed a two-dimensional infrared spectrometer employing fast mechanical scanning and intrinsic phasing of the resulting spectra, leading to a lower sensitivity limit of similar to 100 mu OD level samples. Using this approach, we quantify the biomolecular recognition between a PDZ2 domain and two Aha-mutated peptides. It is shown that this method can distinguish different binding modes and that the energetics of binding can be determined.

DOI: https://doi.org/10.1021/acs.jpclett.7b00742

Quantifying Biomolecular Recognition with Site-Specific 2D Infrared Probes

Philip J. M. Johnson[†], Klemens L. Koziol[†], Peter Hamm

Department of Chemistry,

University of Zurich, Zurich, Switzerland

[†]*these authors contributed equally*

(Dated: May 4, 2017)

Abstract

Azidohomoalanine (Aha) is an unnatural amino acid containing an infrared active azido side chain group which can, through frequency shifts of the azido stretch vibration, act as a probe of local structure. To realize the potential of such structural probes for protein science, we have developed a two-dimensional infrared spectrometer employing fast mechanical scanning and intrinsic phasing of the resulting spectra, leading to a lower sensitivity limit of ∼100 μOD level samples. Using this approach, we quantify the biomolecular recognition between a PDZ2 domain and two Aha-mutated peptides. It is shown that this method can distinguish different binding modes, and that the energetics of binding can be determined.

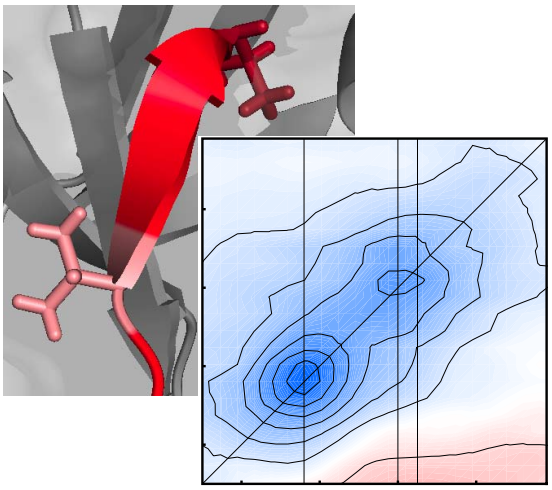

Biomolecular recognition underlies enzymatic activity and signal transduction pathways in effectively all cellular processes, where the energetics of molecular recognition in combination with local concentrations determine the likelihood of protein-protein or protein-ligand binding, and therefore the probability of occurrence of different cellular processes. Knowing these energetics is necessary to understand both the native biochemistry of the cell, and to identify, design, and characterize new drugs with which to control cellular function[1]. Quantifying biomolecular recognition has commonly been the domain of isothermal titration calorimetry (ITC), where the heat of binding between a protein and ligand is monitored as a function of their relative molar ratio[2]. While not a direct measure of structural interactions, through prior knowledge of the binding properties of the biomolecules of interest, it is possible to recover the free energy, enthalpy, and entropy of a binding event[2–4]. Alternative approaches to measuring protein-ligand interactions, often with greater structural specificity, consist of nuclear magnetic resonance (NMR) spectroscopy (either from the point of view of the protein[5–8] or the ligand[5,9]), x-ray crystallography[10] or scattering[11,12], and mass spectrometry techniques[13–16], among many others, each with their own strengths, weaknesses, and applicable affinity regimes[1].

Here, we propose the use of unnatural amino acids with infrared activity in combination with two-dimensional infrared spectroscopy (2D IR) as a means of quantifying equilibrium protein-protein or protein-ligand interactions. Various unnatural amino acids with infrared active side chains have been developed[17–21], which have proven to be sensitive reporters of local structural changes (e.g. protein folding[19] or dynamics[22–24]). In contrast with thermodynamic approaches, single point mutations to infrared-active unnatural amino acids allow for site-specific, and thus structural, information regarding biomolecular recognition[25]. However, experimental limitations have to now hampered the general applicability of this method. The molecular vibrations of nitrile- or azido-modified amino acids have central frequencies in the range of 2100–2300 cm^{-1}, a spectral region free of native protein vibrations, but with significant H_2O or D_2O solvent response[26]. Among the various IR active amino acids, Azidohomoalanine (Aha) may be the most versatile, since it can be incorporated into a protein at essentially any position using a Met auxotrophic expression strategy without the need of an additional chemical modification after protein expression[27]. As a relatively strong absorber with an extinction coefficient of $\sim$300 M^{-1} cm^{-1}[25], the Aha signal is nevertheless still miniscule compared to the solvent response due to the inability to concentrate most

proteins beyond ∼1 mM. In contrast, the water extinction coefficients in this spectral region are some two orders of magnitude smaller, but at a concentration of ∼56 M. The reliable extraction of information pertaining strictly to the protein is thus a significant challenge, particularly with linear infrared spectroscopy.

2D IR spectroscopy[28], a vibrational analogue of 2D NMR spectroscopy, offers a compelling solution to the signal amplitude mismatch described above. As a nonlinear spectroscopy, 2D IR signals scale quadratically with the extinction coefficient, in contrast with the linear nature of FTIR. This acts to significantly enhance the infrared response of the unnatural amino acid vibration with respect to the broad H_2O or D_2O solvent response in a 2D spectrum. Nevertheless, background subtraction of the buffer response is still critical to reliably isolate the Aha signal, and a host of experimental and data processing techniques have been employed in concert to make that possible (see Supporting Information for additional details). First, a syringe pump sample delivery system together with a flow cell was used to exchange sample and buffer solutions multiple times with minimal perturbation to the interferometer. Second, we use the boxcars geometry, which as a background-free method offers the highest possible sensitivity[28], in comparison to the experimentally easier pump-probe geometry[29,30]. Third, fast mechanical scanning of the coherence time delays, taking only ≈0.1 s per single scan, effectively reduces the laser noise, which is not δ-correlated but has a typical correlation time in the order of 1 s.[29]. Fast scanning is implemented through voice coil scanning stages, allowing for the acquisition of data at the Nyquist frequency of the mid-IR field between each successive laser shot (see Fig. S1). Fourth, the deleterious effects of laser scattering are minimized through the use of quasi phase-shifting of the initial coherence time pulses[31]. Finally, inherent phasing of the heterodyne-detected 2D IR spectra[32] is performed using the solvent response as a reference, allowing for precise phasing of each measurement independently (see Fig. S2). These concerted efforts have led to a lower limit of sensitivity of ∼100 μM of Aha, a concentration resulting in a linear optical density of merely ∼100 μOD (in a cuvette with ∼25 μm path length) for the azido stretch vibration[33]. We demonstrate here that binding interactions with dissociation constants on the order of 10^{-5} M and larger become accessible to IR methods with such instrumentation.

To that end, we study the equilibrium binding of two Aha-mutated peptides (i.e., Val(-0)Aha and Val(-3)Aha), derived from the Ras-associating guanine nucleotide exchange factor 2 (RA-GEF), to a PDZ2 domain from the protein tyrosine phosphatase 1E[34,35]. PDZ2

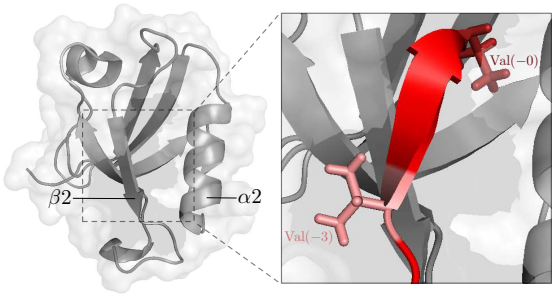

FIG. 1: The PDZ2 domain from the human tyrosine phosphatase 1E (PDB ID 3LNY). Left: the protein consists of six β-strands and two α-helices, with a recognition domain in the groove formed between $\alpha 2$ and $\beta 2$. Right: the wild type RA-GEF peptide ligand forms an extended β-sheet through interaction with $\beta 2$. Also shown are the two mutation sites considered in this work, the C-terminal Val(-0) and Val(-3).

domains consist of six β-strands and two α-helices, structured such that a binding groove spans strand $\beta 2$ and helix $\alpha 2$ (see Fig. 1), and biomolecular recognition occurs primarily through interactions with the C-terminus of target proteins[36–38] in a 1:1 stoichiometry[39]. Assuming that the structure of the bound ligand remains the same upon mutation, the Aha side chain is expected to be buried in the hydrophobic recognition pocket of the binding groove in the case of Val(-0)Aha, but points outward in Val(-3)Aha (see Fig. 1). Previous 2D IR experiments support that structural picture[25].

To determine the binding affinity directly from the infrared response of the Aha-mutated ligands, a series of 2D IR experiments were performed, fixing the initial free ligand concentration (and thus also the Aha concentration) at 500 μM and varying the PDZ2 concentration (see Fig. 2a,c). 2D IR spectra of uncoupled vibrational modes consist of two peaks of opposite sign, related to the transition between the ground and first excited state of the vibrator (0–1 transition, shown in blue in Fig. 2a,c) and the transition between the first and second excited state (1–2 transition, in red)[28]. Here, we focus on the 0–1 transition, which is found along the diagonal of the 2D spectrum, while the 1–2 transition is off-diagonal and for the most part outside the spectral window shown in Fig. 2a,c. The 0–1 signal along the diagonal, which has been extracted in Fig. 2b,d, is free from overlapping contributions of the 1–2 band, allowing for an unambiguous measure of the population of the corresponding ensemble.

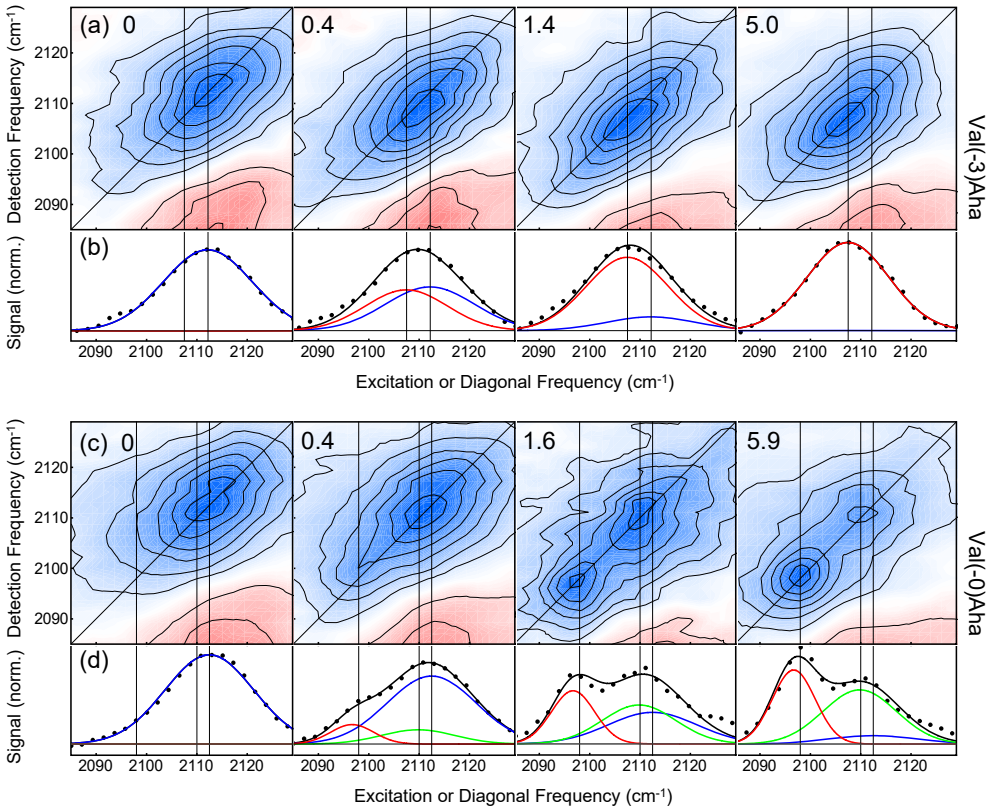

FIG. 2: Biomolecular recognition observed with 2D IR spectroscopy. (a) Sequence of 2D IR spectra of Aha in Val(-3)Aha as a function of molar ratio of PDZ2:peptide, as indicated in the top left of each spectrum. (b) Quantification of the bound and unbound peptide fractions through fitting the diagonal response to a sum of two Gaussians; in blue for the unbound peptide and in red for the tightly bound peptide. Panels (c,d) show the same for Val(-0)Aha, for a which a 3rd component related to an encounter complex is added in green. The vertical lines mark the central frequencies of the various contributions and are shown to guide the eye.

The results for Val(-3)Aha are shown in Fig. 2a,b. With no PDZ2 domain present (leftmost panel), we observe a broad peak at ∼2112 cm^{-1} due to the Aha in the unbound peptide. With increasing molar ratio of the PDZ2 domain, the band initially broadening and gradual shifts towards ∼2107 cm^{-1} due to binding of the ligand to the protein. Binding is essentially saturated already at a molar ratio of 1.4, with minimal deviations up to a molar ratio of 5. For a global fitting of the data, we first determined the central frequencies and widths of two Gaussian distributions of unbound and fully bound ligand, respectively, from the data at molar ratios 0 (Fig. 2b, leftmost panel) and 5 (Fig. 2b, rightmost panel),

and subsequently extracted the amplitudes of these two ensembles as a function of protein concentration. The results of that analysis is shown in Fig. 3a, where the populations are fit to a two-state binding model:

$$P + L \rightleftharpoons PL, \tag{1}$$

revealing a dissociation constant of $K_D = 22 \pm 10$ μM, which is in excellent agreement with that obtained from ITC ($K_D = 33 \pm 5$ μM, see Fig. S3a in Supporting Information).

The results for Val(-0)Aha are richer in content (Fig. 2c,d). With no PDZ2 domain present, the spectrum is essentially the same as for Val(-3)Aha with a center-frequency of 2112.5 cm^{-1}. With increasing molar ratio of the PDZ2 domain, an additional band is observed, initially appearing as an elongation of the band to lower frequencies (molar ratio 0.4), and then evolving into a second distinct red-shifted band at $\sim$2097 cm^{-1} at molar ratios 1.6 and beyond. However, the original band doesn't disappear even at the highest protein concentration, as one might expect, instead, a careful inspection of the 2D IR spectra reveals a small frequency red-shift of that peak of about 2.5 cm^{-1} (see vertical lines in Fig. 2c,d). It has been shown that the Aha frequency reflects the degree of solvation[19], hence we can conclude that the three peaks represent the following conformations: at 2112.5 cm^{-1}, the unbound and random coiled peptide, where the broad line shape is indicative of a heterogeneous local solvent environment; at 2110 cm^{-1}, a loosely bound peptide with a solvated side chain such that the azido group experiences a similarly heterogeneous local environment as in the unbound case; and at 2097 cm^{-1}, a more tightly bound peptide with the side chain buried in the hydrophobic recognition pocket, where the lack of solvent exposure leads to a more homogeneous local environment and thus a narrow line shape.

Recent molecular dynamics simulations of the binding of the wild-type peptide to the PDZ2 domain[38] suggest that the loosely bound peptide is in fact an encounter complex, in which the ligand is not yet bound inside the binding groove. Rather, stabilized by non-native salt bridges formed with residues from α2 and β2, the ligand spans across the binding groove (see Fig. 6 of Ref.[38]). In such an encounter complex, the Aha label remains solvated to almost the same extent as in the unbound peptide, leading to the only minor frequency shift of its vibration. This assignment suggests a model:

$$P + L \rightleftharpoons PL_1 \rightleftharpoons PL_2, \tag{2}$$

with a dissociation constant of the encounter complex $K_{D1} \equiv [P][L]/[PL_1]$ and an equilib-

rium constant between encounter complex and tightly bound peptide $K_{12} \equiv [PL_2]/[PL_1]$. A fit as for Val(-3)Aha turned out to be under-determined in this case, because of the three overlapping distributions with a very small frequency shift of unbound peptide *vs.* encounter complex and the fact that binding is not completely saturated even at a molar ratio 5.9. Rather, we included the model Eq. 2 in a single global fitting step of the complete data set, thereby fixing the relative amplitudes of the three contributions as a function of protein concentration to the model (see Supporting Information for details). This procedure rendered the fit stable and revealed $K_{D1} = 470 \pm 100$ μM and $K_{12} = 0.8 \pm 0.2$ (Figs. 2d and 3b).

To connect these results to ITC, which cannot distinguish the two binding modes and thus measures the combined effect of both, we note that model Eq. 2 is mathematically identical to model Eq. 1 when replacing $[PL] \equiv [PL_1] + [PL_2]$ and defining an overall dissociation constant:

$$K_D^{all} \equiv \frac{[P][L]}{[PL_1] + [PL_2]} = \frac{K_{D1}}{1 + K_{12}}. \tag{3}$$

With that, we obtain $K_D^{all} = 250 \pm 50$ μM, again in excellent agreement with the ITC result of 250 ± 60 μM (see Fig. S3b in Supporting Information).

It is the C-terminal carboxyl group together with the hydrophobic interactions of the Val(-0) side chain in the recognition pocket that is mostly responsible for binding[36–38]. Consequently, mutation of Val(-0) with the longer and weakly polar Aha side chain, which is still buried in the hydrophobic recognition pocket according to the 2D IR results, destabilizes the tightly bound state, as evidenced by the rather large K_D^{all} (250 ± 50 μM). This, in turn, increases the relative population of the encounter complex so that it becomes experimentally observable. Val(-3)Aha, on the other hand, has a much larger binding affinity ($K_D = 22 \pm 10$ μM), similar to that of the wild type peptide. Based on the high binding affinity, we may assume that the structure in the binding groove is the same as the wild type (Fig. 1), hence, the Aha label points outwards and thus is solvated to a significant extent even if the ligand is tightly bound. We therefore would not be able to spectroscopically distinguish the tightly bound peptide from an encounter complex. However, when assuming that the dissociation constant K_{D1} of the encounter complex is about the same in both mutants (since it binds less specifically), we can still conclude from Eq. 3 that the encounter complex is hardly populated in Val(-3)Aha.

The spectroscopic approach proposed here is similar to NMR[5–9] with a "chemical shift"

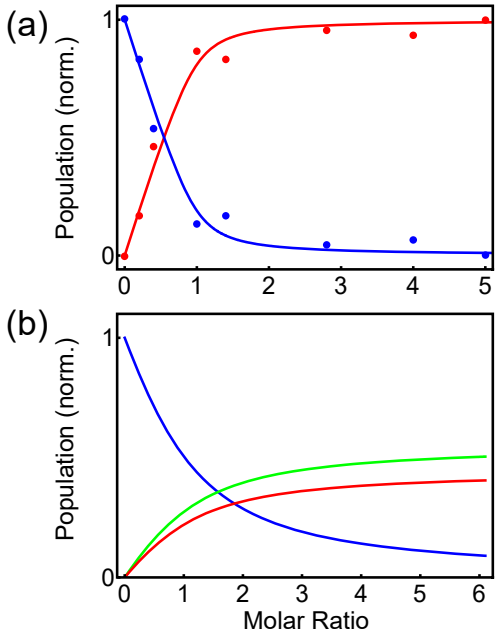

FIG. 3: Normalized amplitudes of the various states of (a) Val(-3)Aha and (b) Val(-0)Aha as a function of molar ratio of PDZ2:peptide. In panel (a), the population of the unbound peptide is shown in blue and that of the bound peptide in red together with a fit based on the model Eq. 1. Panel (b) shows in addition the population of the encounter complex in green with a fit based on the model Eq. 2. The fitting strategies are different in both cases, as discussed in the text and in Supporting Information.

that reports on the environment of a spectroscopic probe. In the affinity regime of the system studied here, NMR would be in the limit of coalescing lines[40], in which case only one band is observed, whose frequency position reflects the average over all states. While methods based on relaxation dispersion have been developed to recover exchange rates and chemical shift of those "invisible states"[40,41], 2D IR is inherently an ultrafast spectroscopy, and coalescence will not occur for any process slower than ∼1 ps. This is why, in the present study, the three states of Val(-0)Aha indeed reveal three bands. Both spectroscopic techniques, NMR and 2D IR, are thus complementary.

While the technical challenges of measuring weak infrared signals have to now limited the application of IR methods in biomolecular recognition, these measurements pave the way for greater adoption of unnatural amino acids as infrared probes for protein-protein and protein-ligand interactions. Different vibrational labels that respond more strongly to the

environment, such as ester groups in non-natural amino acid side chains[21], might be able to resolve even more binding modes. Furthermore, with recent advances in high repetition rate amplified laser systems, multidimensional IR spectroscopy of equilibrium biomolecular recognition will be accessible within seconds[42,43], allowing for the collection of a complete binding interaction curve in a fraction of the time needed for thermodynamic measures of binding, while simultaneously yielding greater structural information reflecting possible conformational heterogeneity. These measurements also serve as a proof of principle for the application of unnatural amino acids to non-equilibrium experiments, in which an actinic pump pulse initiates a structural process such as ligand unbinding, which is then followed by transient 2D IR spectroscopy[44]. Together with similar sensitivity requirements as in the present case, the observation of such non-equilibrium processes will need the fast intrinsic time-resolution of 2D IR spectroscopy, the critical feature distinct from established methods used to determine biomolecular recognition

Acknowledgments: We thank Rolf Pfister for help with peptide synthesis, Marjorie Sonnay for help with peptide purification, Ilian Jelesarov for very valuable discussions regarding the ITC measurements, Steven Waldauer for the ITC data of Val(-3)Aha, Robbert Bloem and Brigitte Stucki-Buchli for contributions at an early stage of this project, and Oliver Zerbe, Amedeo Caflisch and Ben Schuler for helpful discussions on various other aspects of the work. The work has been supported in part by a European Research Council (ERC) Advanced Investigator Grant (DYNALLO), and by the Swiss National Science Foundation (SNF) through the NCCR MUST as well as Grant 200021_165789/1.

Supporting Information Available: Details on the protein expression and peptide synthesis, the 2D-IR experimental setup including a demonstration of the advantage of fast scanning and the intrinsic phasing, the fitting procedure, as well as the ITC measurements are given in Supporting Information.

---

[1] Renaud, J.-P.; Chung, C.; Danielson, U. H.; Egner, U.; Hennig, M.; Hubbard, R. E.; Nar, H. Biophysics in drug discovery: impact, challenges and opportunities, *Nat. Rev. Drug Discovery*

2016, *15*, 679–698.

[2] Freyer, M. W.; Lewis, E. A. Isothermal titration calorimetry: experimental design, data analysis, and probing macromolecule/ligand binding and kinetic interactions, *Methods Cell Biol.* **2008**, *84*, 79–113.

[3] Turnbull, W. B.; Daranas, A. H. On the Value of c: Can Low Affinity Systems Be Studied by Isothermal Titration Calorimetry?, *J. Am. Chem. Soc.* **2003**, *125*, 14859–14866.

[4] Jelesarov, I.; Bosshard, H. R. Isothermal titration calorimetry and differential scanning calorimetry as complementary tools to investigate the energetics of biomolecular recognition, *J. Mol. Recognit.* **1999**, *12*, 3–18.

[5] Pellecchia, M.; Bertini, I.; Cowburn, D.; Dalvit, C.; Giralt, E.; Jahnke, W.; James, T. L.; Homans, S. W.; Kessler, H.; Luchinat, C.; Meyer, B.; Oschkinat, H.; Peng, J.; Schwalbe, H.; Seigal, G. Perspectives on NMR in drug discovery: a technique comes of age, *Nat. Rev. Drug Discovery* **2008**, *7*, 738–745.

[6] Harner, M. J.; Frank, A. O.; Fesik, S. W. Fragment-based drug discovery using NMR spectroscopy, *J. Biomol. NMR* **2013**, *56*, 65–75.

[7] Wu, B.; Zhang, Z.; Noberini, R.; Barile, E.; Giulianotti, M.; Pinilla, C.; Houghton, R. A.; Pasquale, E. B.; Pellecchia, M. HTS by NMR of combinatorial libraries: a fragment-based approach to ligand discovery, *Chem. Biol.* **2013**, *20*, 19–33.

[8] Wu, B.; Barile, E.; De, S. K.; Wei, J.; Purves, A.; Pellecchia, M. High-throughput screening by Nuclear Magnetic Resonance (HTS by NMR) for the identification of PPIs Antagonists, *Current Topics in Medicinal Chemistry* **2015**, *15*, 2032–2042.

[9] Cala, O.; Guilliere, F.; Krimm, I. NMR-based analysis of protein-ligand interactions, *Anal. Bioanal. Chem.* **2014**, *406*, 943–956.

[10] Blundell, T. L.; Patel, S. High throughput X-ray crystallography for drug discovery, *Curr. Opin. Pharmacol.* **2004**, *4*, 490–496.

[11] Tuukkanen, A. T.; Svergun, D. I. Weak protein-ligand interactions studied by small-angle X-ray scattering, *FEBS J.* **2014**, *281*, 1974–1987.

[12] Vestergaard, B.; Sayers, Z. Investigating increasingly complex macromolecular systems with small-angle X-ray scattering, *IUCrJ* **2014**, *1*, 523–529.

[13] Hofstadler, S. A.; Sannes-Lowery, K. A. Applications of ESI-MS in drug discovery: interrogation of noncovalent complexes, *Nat. Rev. Drug Discovery* **2006**, *5*, 585–595.

[14] Vivat Hannah, V.; Atmanene, C.; Zeyer, D.; Van Dorsselaer, A.; Sanglier-Cianferani, S. Native MS: an 'ESI' way to support structure- and fragment-based drug discovery, *Future Medicinal Chemistry* **2010**, *2*, 35–50.

[15] Chalmers, M. J.; Busby, S. A.; Pascal, B. D.; West, G. M.; Griffin, P. R. Differential hydrogen/deuterium exchange mass spectrometry analysis of protein-ligand interactions, *Expert Rev. Proteomic.* **2011**, *8*, 43–59.

[16] Konermann, L.; Pan, J.; Liu, Y. H. Hydrogen exchange mass spectrometry for studying protein structure and dynamics, *Chem. Soc. Rev.* **2011**, *40*, 1224–1234.

[17] Getahun, Z.; Huang, C.-Y.; Wang, T.; De Leon, B.; DeGrado, W. F.; Gai, F. Using Nitrile-Derivatized Amino Acids as Infrared Probes of Local Environment, *J. Am. Chem. Soc.* **2003**, *125*, 405–411.

[18] Cho, K.-I.; Lee, J.-H.; Joo, C.; Han, H.; Cho, M. β-Azidoalanine as an IR Probe: Application to Amyloid Aβ(16-22) Aggregation, *J. Phys. Chem. B* **2008**, *112*, 10352–10357.

[19] Taskent-Sezgin, H.; Chung, J.; Banerjee, P. S.; Nagarajan, S.; Dyer, R. B.; Carrico, I.; Raleigh, D. P. Azidohomoalanine: A Conformationally Sensitive IR Probe of Protein Folding, Protein Structure, and Electrostatics, *Ang. Chem. Int. Ed.* **2010**, *49*, 7473–7475.

[20] Ma, J.; Pazos, I. M.; Zhang, W.; Culik, R. M.; Gai, F. Site-Specific Infrared Probes of Proteins, *Annu. Rev. Phys. Chem.* **2015**, *66*, 357–377.

[21] Pazos, I. M.; Ghosh, A.; Tucker, M. J.; Gai, F. Ester carbonyl vibration as a sensitive probe of protein local electric field, *Angew. Chemie - Int. Ed.* **2014**, *53*, 6080–6084.

[22] Ye, S.; Zaitseva, E.; Caltabiano, G.; Schertler, G. F. X.; Sakmar, T. P.; Deupi, X.; Vogel, R. Tracking G-protein-coupled receptor activation using genetically encoded infrared probes, *Nature* **2010**, *464*, 1386–1389.

[23] Chung, J. K.; Thielges, M. C.; Fayer, M. D. Conformational Dynamics and Stability of HP35 Studied with 2D IR Vibrational Echoes, *J. Am. Chem. Soc.* **2012**, *134*, 12118–12124.

[24] Blasom, E. J.; Maj, M.; Cho, M.; Thielges, M. C. Site-Specific Characterization of Cytochrome P450cam Conformations by Infrared Spectroscopy, *Anal. Chem.* **2016**, *88*, 6598–6606.

[25] Bloem, R.; Koziol, K.; Waldauer, S. A.; Buchli, B.; Walser, R.; Samatanga, B.; Jelesarov, I.; Hamm, P. Ligand Binding Studied by 2D IR Spectroscopy Using the Azidohomoalanine label, *J. Phys. Chem. B* **2012**, *116*, 13705–13712.

[26] Max, J.-J.; Chapados, C. Isotope effects in liquid water by infrared spectroscopy. III. H_2O and

D_2O spectra from 6000 to 0 cm^{-1}, *J. Chem. Phys.* **2009**, *131*, 184505.

[27] Kiick, K.; Saxon, E.; Tirrell, D.; Bertozzi, C. Incorporation of azides into recombinant proteins for chemoselective modification by the Staudinger ligation, *Proc. Natl. Acad. Sci. U.S.A.* **2002**, *99*, 19.

[28] Hamm, P.; Zanni, M. Concepts and Methods of 2D Infrared Spectroscopy, *Cambridge University Press* **2011**.

[29] Helbing, J.; Hamm, P. Compact implementation of Fourier transform two-dimensional IR spectroscopy without phase ambiguity, *J. Opt. Soc. Am. B* **2011**, *28*, 171–178.

[30] Shim, S. H.; Zanni, M. T. How to turn your pump-probe instrument into a multidimensional spectrometer: 2D IR and Vis spectroscopies via pulse shaping, *Phys. Chem. Chem. Phys.* **2009**, *11*, 748–761.

[31] Bloem, R.; Garrett-Roe, S.; Strzalka, H.; Hamm, P.; Donaldson, P. Enhancing signal detection and completely eliminating scattering using quasi-phase-cycling in 2D IR experiments, *Opt. Express* **2010**, *18*, 27067–27078.

[32] Johnson, P. J. M.; Koziol, K. L.; Hamm, P. Intrinsic phasing of heterodyne-detected multidimensional infrared spectra, *Opt. Express* **2017**, *25*, 2928–2938.

[33] Koziol, K. L.; Johnson, P. J. M.; Stucki-Buchli, B.; Waldauer, S. A.; Hamm, P. Fast infrared spectroscopy of protein dynamics: advancing sensitivity and selectivity, *Curr. Opin. Struc. Biol.* **2015**, *34*, 1–6.

[34] Jemth, P.; Gianni, S. PDZ Domains: folding and binding, *Biochemistry* **2007**, *46*, 8701–8708.

[35] Chi, C. N.; Bach, A.; Strømgaard, K.; Gianni, S.; Jemth, P. Ligand binding by PDZ domains, *Biofactors* **2012**, *38*, 338–348.

[36] Doyle, D. A.; Lee, A.; Lewis, J.; Kim, E.; Sheng, M.; MacKinnon, R. Crystal structures of a complex and peptide-free membrane protein-binding domain: molecular basis of peptide recognition, *Cell* **1996**, *85*, 1067–1076.

[37] Songyang, Z.; Fanning, A. S.; Fu, C.; Xu, J.; Marfatia, S. M.; Chishti, A. H.; Crompton, A.; Chan, A. C.; Anderson, J. M.; Cantley, L. C. Recognition of unique carboxy-terminal motifs by distinct PDZ domains, *Science* **1997**, *275*, 73–77.

[38] Blöchliger, N.; Xu, M.; Caflisch, A. Peptide Binding to a PDZ Domain by Electrostatic Steering via Nonnative Salt Bridges, *Biophys. J.* **2015**, *108*, 2362–2370.

[39] Milev, S.; Bjelić, S.; Georgiev, O.; Jelesarov, I. Energetics of peptide recognition by the second

PDZ domain of human protein tyrosine phosphatase 1E, *Biochemistry* **2007**, *46*, 1064–1078.

[40] Baldwin, A. J.; Kay, L. E. NMR spectroscopy brings invisible protein states into focus, *Nat. Chem. Biol.* **2009**, *5*, 808–814.

[41] Mittermaier, A.; Kay, L. E. New tools provide new insights in NMR studies of protein dynamics, *Science* **2006**, *312*, 224–228.

[42] Luther, B. M.; Tracy, K. M.; Gerrity, M.; Brown, S.; Krummel, A. T. 2D IR Spectroscopy at 100 kHz Utilizing a Mid-IR OPCPA Laser Source, *Opt. Express* **2016**, *24*, 4117–4127.

[43] Greetham, G. M.; Donaldson, P. M.; Nation, C.; Sazanovich, I. V.; Clark, I. P.; Shaw, D. J.; Parker, A. W.; Towrie, M. A 100 kHz Time-Resolved Multiple-Probe Femtosecond to Second Infrared Absorption Spectrometer, *Appl. Spectrosc.* **2016**, *70*, 645–653.

[44] Kolano, C.; Helbing, J.; Kozinski, M.; Sander, W.; Hamm, P. Watching hydrogen bond dynamics in a β-turn by transient two-dimensional infrared spectroscopy, *Nature* **2006**, *444*, 469–472.